

RSC Advances



This is an *Accepted Manuscript*, which has been through the Royal Society of Chemistry peer review process and has been accepted for publication.

Accepted Manuscripts are published online shortly after acceptance, before technical editing, formatting and proof reading. Using this free service, authors can make their results available to the community, in citable form, before we publish the edited article. This *Accepted Manuscript* will be replaced by the edited, formatted and paginated article as soon as this is available.

You can find more information about *Accepted Manuscripts* in the [Information for Authors](#).

Please note that technical editing may introduce minor changes to the text and/or graphics, which may alter content. The journal's standard [Terms & Conditions](#) and the [Ethical guidelines](#) still apply. In no event shall the Royal Society of Chemistry be held responsible for any errors or omissions in this *Accepted Manuscript* or any consequences arising from the use of any information it contains.

A Revised Paper Submitted to the

RSC Advanced

**Oxygen Sensor Utilizing Ultraviolet Irradiation Assisted ZnO
Nanorods under Low Operation Temperature**

Chen-Shiun Chou¹, Yung-Chen Wu^{1,2}, and Che-Hsin Lin¹

¹Department of Mechanical and Electro-Mechanical Engineering, National Sun Yat-sen
University, Kaohsiung, Taiwan, 804 ROC

² Metal Industries Research & Development Centre, Kaohsiung, Taiwan, 811 ROC

Corresponding author: Prof. Che-Hsin Lin

e-mail: chehsin@mail.nsysu.edu.tw

Tel: +886-7-5252000-4240

Fax: +886-946-526044

*The preliminary results of the present study have been reported at The 8th Annual IEEE International Conference on Nano/Micro Engineered and Molecular Systems (IEEE NEMS 2013), Suzhou, China, Apr. 7-10, 2013.

ABSTRACT

This paper presents a novel ultraviolet (UV) irradiation assisted nanostructured ZnO film for high performance oxygen sensing under a low working temperature. Nanorod ZnO structures with high exposing area are synthesized on a glass substrate with interdigital sensing electrodes utilizing the developed two-stage sol-gel and hydrothermal processes. A UV-LED with the emission wavelength of 370 nm is then used to enhance the sensing performance of the nanostructured ZnO film. The oxygen sensor can work at a temperature of 50°C while with the assist of UV irradiation. The response of the UV-assisted ZnO film shows 4.66 times larger than the same film without UV exposure. The method developed in the present study provides a simple yet high performance method for oxygen sensing under low operation temperature.

Keywords: UV-LED; Nanorod ZnO; Oxygen sensor; Sol-gel; Hydrothermal

I. INTRODUCTION

Oxygen is one of the most important elements required to sustain life as it plays the roles in respiration and oxidation for all living things. The monitoring of the environmental oxygen content is essential in various fields including the medicine, aquaculture, farming, chemical industries and fuel combustion [1, 2]. The ambient oxygen concentration is also considered as a safety factor for industrial applications [3]. For example, high ambient oxygen level is risky for explosive but low oxygen content can cause gas poisoning for underground engineers. The dissolved oxygen concentration in water is typically maintained in about 5 - 8 ppm for aquaculture applications.[4] Therefore, there is an urgent demand for developing high performance and cost-efficient oxygen sensors. Oxygen concentration in an environment can be determined with various measuring principles including the electrochemical redox detections or the solid-state sensors.[2, 5, 6] Over these sensing methods, solid-state ceramic films such as metal oxides fabricated with vapor deposition processes are the most promising approach for producing commercial oxygen sensors [7]. These devices have several advantages including low cost, small size, easy to integrate with electronic circuit and relatively low power consumption.

Semiconductor-based metal oxides have been used for gas sensing since 1962, when Seiyama *et al.* used a thin layer of zinc oxide to detect volatile organic compounds (VOC) of propane and n-butane[8]. Inspired by the work, a number of metal oxide layers such as TiO₂[9-11], SnO₂[12-14] and In₂O₃[15, 16] were used as the sensing materials for various gases detections. However, metal oxide-based gas sensors usually rely on a high working temperature to enhance catalytic properties of the metal oxides for gas sensing.[REF] The high working temperature for this kind of sensor consumes more energy for heating the

sensing element and also reduces the lifetime of the sensor. On contrast, the sensing performance of these metal-oxide based sensors dramatically decreases at lower working temperatures. Therefore, a number of methods have been developed to enhance the sensing performance of the metal-oxide based gas sensors. Modifying the metal oxide layer by doping a trace amount of transient metal such as Cr, Fe or Pd is the most simple and straight forward way to enhance the sensing performance of these sensors[17-19]. Introducing the structural defects into the material matrix to increase the carrier mobility using the heterogeneous structure [20-22] or producing porous structures to increase the exposed sensing area [23, 24] are also common approaches for sensing performance enhancement. For example, metal oxide layer comprising a ZnO/SnO₂ hetero-contact interface was used for detecting CO was reported[25]. Chen *et al.*[26] used the α -Fe₂O₃/SnO₂ core-shell structure for ethanol detection at an operating temperature of 220°C. Recently, a Pd-doped SnO₂ was reported to detect formaldehyde of the concentration as low as 50 ppb at 190°C [27]. These approaches were capable of enhancing the detection performance of the gas sensors in a simple way. However, the fabrication for the heterogeneous structured metal oxides usually needs a high sintering temperature. Moreover, these gas sensors also required a relative high working temperature (higher than 150°C) to reach the catalytic temperature [6]. Nanostructured metal oxides were popular to be employed in producing high performance sensors due to their excellent catalytic behaviors and high surface-to-volume ratio. The sensing performance of these gas sensors was greatly enhanced and the working temperature was also significantly reduced. Nevertheless, this work is to further enhance the performance of the nanostructured ZnO metal oxide sensing layer.

Ultraviolet (UV) is a high energy beam with the photon energies from 3.0 to 12.4 eV (400 nm – 10 nm) which is overlapped with the band gap of zinc oxide (around 3.4 eV) [28].

Therefore, UV exposure can be an efficient way to excite the hole-electron pairs in the sensing materials, such that the measured resistance of the semiconductor metal oxides is significantly reduced [29]. Recently, the interaction between with light irradiation with ZnO surface was investigated [30]. The light-induced electrons in ZnO may attract the high electron negativity molecules, such as oxygen or fluorine, and minimized the mobility of the electrons. The resistance of the sensing material increases with the increasing amount of the attracted oxygen molecules [31]. In this regards, UV irradiation can enhance the sensing performance of the gas sensors without using the high working temperature to produce the electron-hole pairs. With this sensing mechanism, there are a number of researches have demonstrated to use nanostructured ZnO layer with UV radiation for gas sensing in the recent years. For example, Peng *et al* reported a ZnO nanorod-based formaldehyde sensor with a 120-fold sensitivity enhancement under UV exposure[32]. However, the nanorod structured ZnO was grown parallel to the substrate surface such that the exposed surface area was limited. Fan *et al.*[33] presented the used of packed polycrystalline ZnO nanoparticles for NO₂. Results showed that the ppm-level of NO₂ could be detected with the assistance of UV exposure. Nevertheless, the fabrication process for packing the ZnO nanoparticles into a line trench was delicate and time-consuming.

In order to enhance the sensing performance under low operation temperature, this study reports a simple and reliable method to produced out-of-plane ZnO nanorods for oxygen detection. The grass-like ZnO structure is produced with a two-stage sol-gel and hydrothermal process. The high exposed area of the out-of-plane ZnO nanorod greatly enhances the UV exposure efficiency. On contrast, a lower dark current can be obtained due to small contact area to the substrate electrode [34]. Therefore, the resistance change due to the UV exposure is greatly increased such that oxygen detection can be achieved without applying a high

working temperature. The surface morphology of ZnO nanostructures and the sensing performance produced with different ZnO producing processes are systematically inspected in the present study. The repeatability of the developed oxygen sensor utilizing UV-assisted ZnO nanorods is also experimentally measured to evaluate the performance of the oxygen sensor under a low working temperature.

II. MATERIALS AND METHODS

A. Sensing mechanism

Figure 1 presents the working principle of the proposed oxygen sensing method. The high exposed area of the nanostructured ZnO sensing layer is beneficial for high efficient carrier induction. The UV irradiation on the ZnO nanostructures can induce the excited electrons on the material surface and reduce the resistance of the sensing layer. The mechanism regarding the photoelectric response of the nanostructured ZnO is related to the surface adsorbed species and the volume process.[35] The oxygen molecules are attracted by the UV induced electrons and form O_2^- (ads) due to the greater electronegativity.[36] The conductivity of the ZnO is then decreased due to the decreasing electron carriers in the sensing layer, resulting in a increasing measured resistivity. In contrast, the ZnO nanorods without applying UV exposure surface exhibited fewer electrons, resulting in a lower affinity for oxygen molecules adsorbing onto the surface of ZnO nanorods. In general, the decreased conductivity is promotional to the adsorbed oxygen molecules on the surface of nanostructured ZnO. High performance oxygen detection can be achieved at a low working temperature with the assistance of UV irradiation.

B. Chip fabrication and Synthesis of nanostructured ZnO

Figure 2 presents the fabrication process of the oxygen sensing chip. A low-cost soda-lime glass was used as the substrate for developed oxygen sensor. Interdigital sensing electrodes were patterned with a standard photolithography process and metal etching process (Fig. 2A). Chromium and gold metal layers with the thicknesses of 500 Å and 2000 Å were first deposited on the glass substrate, respectively. The substrates were spin-coated with AZ4620 photoresist and soft-baking at 100°C for 3 min. The interdigital area was patterned using a standard UV lithography process. The patterned substrate was then immersed into the developer (AZ400K: DI water = 1:3). After rinsing DI water, the substrates were immersed into gold etchant (Type TFA). The substrates were rinsed in DI water and immersed into chromium etchant (Cr-7T). After finishing metal etching, the photoresist layer was removed with acetone to expose the metal electrodes (Fig. 2B). The nanostructured ZnO sensing layer were synthesized on a substrate with interdigital electrodes by the sol-gel process to form the ZnO seed layer and then a hydrothermal process to grow the grass-like ZnO nanorods. The reagents of zinc acetate ($\text{Zn}(\text{CH}_3\text{COO})_2 \cdot 2\text{H}_2\text{O}$) and hexamethylenetetramine ($\text{C}_6\text{H}_{12}\text{N}_4$) were purchased from Panreac-Quimica (Barcelona, Spain). Ethanolamine ($\text{C}_2\text{H}_7\text{NO}$) was purchased from Sigma-Aldrich (Louis, USA). Methanol (CH_4O) was obtained from Echo Chemical Co., Ltd. (Miaoli, Taiwan). All of the chemical reagents and solvents were of an analytical grade. A 0.1 M of precursor solution prepared by dissolving 2×10^{-3} moles of zinc acetate in 20 ml of methanol. Once the solution was prepared, ethanolamine of 2×10^{-3} moles was added into this precursor solution. The solution was then stir-mixed and heated at 60°C for 1 hour and stored for one day. The ZnO precursor solution was spun onto a substrate with interdigital electrode with 1000 rpm for 20 s and then baked at 100°C for 10 min. (Fig.2C) The spun substrate with ZnO precursor was sintered in at 200°C for 30 min then ramped to 400°C for 0.5 hour to form the ZnO seed layer on the substrate with interdigital electrodes.(Fig. 2D) After producing the

seed layer, the substrate was then immersed into a mixed solution composed of 10^{-2} M zinc acetate and 10^{-2} M hexamethyltetramine for hydrothermally growing the ZnO nanorods. The hydrothermal process was kept at 90°C for 30 minutes to grow ZnO nanorods from the seeds. (Fig. 2E) The substrate was finally cleaned with 95% alcohol followed by DI water and then dried on a hotplate. (Fig. 2F)

C. Oxygen detection

The sensing performance including the resistance response and time response of the produced ZnO-based oxygen sensor were characterized in a home-built chamber. An 1 W UV-LED with the major emission wavelength of 370 nm was used to enhance the sensing performance of the developed sensor. The measured surface irradiance on the sensor surface was 0.15 mW/cm^2 . The resistance change of the sensing layer was measured using a LCR meter (U1732C, Agilent, USA). The measured frequency for resistance response of the oxygen sensor was set at 1 kHz. The measured resistance was acquired and recorded using a PC via an IR-USB connecting cable. For measuring the resistance response, the chamber was first pumped to 5×10^{-2} mTorr and then set to the desired oxygen concentration by injecting pure oxygen and pure nitrogen into the chamber by means of a mass flow controller (MFC). The sensing performance of the sensors was evaluated with a defined parameter “Response”.

$$Response = \frac{\Delta R}{R_0} \times 100\% \quad (1)$$

Where R_0 is with the initial resistance of the sensor and ΔR is with the measured resistance change corresponding to the change of oxygen concentration. The sensitivity (S) was defined as the ratio of $Response/\Delta\% \text{ O}_2$ to further quantitatively evaluate the sensing performance of the developed sensors. The equation for the definition of sensitivity is

described below, where $\Delta\% \text{ O}_2$ was the change of the oxygen concentration.

$$\text{Sensitivity} = \frac{\text{Response}}{\Delta\% \text{ O}_2} \quad (2)$$

III. RESULTS AND DISCUSSION

Figure 3 shows the XRD patterns of the synthesized ZnO nanorod layer for oxygen detection. The diffraction peaks for 2θ at 31.77° , 34.42° , 36.25° , 47.54° , 56.6° , 62.87° and 67.96° indicate the (100), (002), (101), (102), (110), (103), and (112) crystalline planes, respectively. It was found that the crystalline structure of the ZnO nanorods is wurzite structure since the diffraction pattern of the produced ZnO nanorods matches with JCPDS card # 36-1451[37]. The XRD result confirms that the high purity of the produced ZnO nanorods. The high intensity of (002) diffraction peak illustrates that the synthesized ZnO nanorods exhibited significant tendency for growing along the c-axis. Figure 4 shows the close-up view for the surface morphology of the synthesized ZnO nanostructures utilizing various procedures. Figure 4(A) shows the sol-gel grown ZnO seed layer prior to the hydrothermal growth for the nanorods. The SEM image indicated that ultra-fine ZnO nanospheres of the size about 10 nm were deposited on the substrate. Figure 4(B) shows the synthesized ZnO nanospheres by sol-gel method with 0.5 M of precursor bath. A higher precursor concentration resulted in a bigger grown ZnO particle such that the size of these nanospheres was about 20 nm in size. It's also noted that there were some micro-cracks observed on the surface of the grown ZnO layer. These cracks could be formed due to the mismatched thermal expansion coefficient between the substrate and the formed ZnO layer under the high sintering temperature. Figure 4(C) shows the top view image for the surface

morphology of synthesized ZnO nanorods. The SEM image showed that the nanostructured ZnO was uniformly distributed on the substrate and the diameter of grown ZnO nanorods was about 40 nm. The extended surface area of the ZnO nanorods greatly enhanced the exposed area in compare to the nanospheres ZnO sensing layer. Figure 4(D) shows the side-view image of synthesized ZnO nanorods. Results again confirmed the growth direction of the nanorods was perpendicular to the substrate, indicating that the ZnO was grown along the C-axis. It is also noted that the length of ZnO nanorods was about 600 nm.

Figure 5 presents the measured response for exposing the ZnO nanorod sensor into 97% oxygen with and without UV irradiation under different operation temperatures. Results showed that the response of ZnO nanorods with UV irradiation was significantly higher than the same film without UV irradiation at all operation temperatures. The measured results also showed that the UV irradiated ZnO sensing layer exhibited a lower R_0 compared to the same film without UV irradiation. The results supported that the ZnO nanorods surface has more conductive carriers in the sensing layer. It is also noted that the response of the developed oxygen sensor increased with the increasing operation temperature in a certain temperature range, which is similar to other reports[27]. It is also noted that the sensing response of UV-assisted ZnO oxygen sensor decreased while the operation temperature was at 250°C. This might be caused by the thermal expansion induced delamination between the nanostructured ZnO sensing layer and the glass substrate at this high temperature. Figure 6 shows the measured response for detecting 97% oxygen using various ZnO sensing layers with and without UV irradiation at a low operation temperature of 50°C. Results showed that the grass-like ZnO nanorod sensing layer with UV irradiation exhibited the highest response due to its large exposed surface area. The measured response for the UV irradiated ZnO nanorods sensing layer was 419% while the same sensing layer without UV irradiation

showed the response only 74%. Results showed that the UV irradiation enhanced the sensing response for 4.66 times compared to the same sensing layer without UV irradiation. The UV irradiation was an efficient way to enhance the sensing performance of ZnO-based gas sensor. Figure 7 presents the measured time response of various sensing layer with and without UV irradiation at the low working temperature of 50°C. The calculated adsorption (90% response) and desorption times (63% response) for the UV-assisted nanorod ZnO were 286 and 54 s, respectively. Results showed the time response of the developed UV-assisted nanorod ZnO sensing film was much faster than the same sensor without UV irradiation. The changing rate for the electrical resistance of the ZnO nanorods was expected to be faster than the sensing layer without UV irradiation due to its point-junction property of the ZnO layer [38]. Those point junctions in the sensing material provided the potential barriers such that the electrical resistance changed faster while oxygen sensing. In addition, the ZnO nanospheres showed the slowest adsorption behavior due to the aggregation of the ZnO nanoparticles, resulting in a longer diffusion path for oxygen molecules. The repeating tests showed that the developed sensor had good repeatability and stability for oxygen detection. Figure 8 shows three repeating measurement for detecting 97% oxygen to evaluate the repeatability for the developed sensor with UV irradiation. The calculated variation for these three measurements was only 3.3%, indicating nice reproducibility of the ZnO-based oxygen sensor.

Figure 9 shows measured sensing performance of the developed UV-assisted ZnO nanorods for detecting oxygen at a low working temperature of 50°C. Figure 9A shows the continuous measurement for the step response for detecting oxygen of different pressures. Figure 9B presents the relationship between the measured responses and the oxygen pressures. Note that the measurement was performed in a high vacuum chamber under a precise pressure control. Results showed that the nice linearity ($R^2=0.9952$) from 5 to 1000 mTorr was

obtained, confirming the good sensing performance of the developed sensor. Results also indicated that the limit of detection (LOD) for the oxygen sensor was as low as 5 mTorr. The calculated sensitivity of the sensor was 0.17(%/mTorr O₂). The LOD and sensitivity of the developed sensor were 64.4 and 3.1 times greater than the reported cobalt-doped ZnO nanofibres, respectively [39]. Figure 10 presents measured sensing performance of the developed sensor for detecting oxygen concentration at 50°C under 1 atm. Figure 10A shows the measured step response for detecting oxygen of different ratios. Figure 10B presents the relationship between the measured responses under various oxygen ratios. The chamber was purged to 1 atm with the sample gas composed of different oxygen ratios (mixed with pure nitrogen) by means of a precision MFC. Results indicated that nice linearity ($R^2=0.9337$) from 10% to 97% of oxygen ratio was obtained. The calculated sensitivity for the developed oxygen sensor was 1.83(%/% O₂) under 1 atm of measuring condition. The sensitivity of the developed sensor was 3.5 times higher than the SnO₂-gated AlGaN/GaN transistor under 1 atm [40]. In addition, the developed sensor also exhibited the sensitivity about 4.5 times higher than that of the multi-wall carbon nanotubes based oxygen sensor at the same condition [41]. The experimental results confirmed that the wide detection range and good sensing performance for the developed oxygen sensor assisted with UV irradiation. The developed oxygen sensor utilizing UV-assisted ZnO nanorods has shown its potential to be a high performance oxygen sensor which can be operated at a low working temperature.

IV. CONCLUSIONS

A high performance oxygen sensor utilizing UV-assisted ZnO nanorods under a low operation temperature has been developed. A simple two-stage sol-gel and hydrothermal processes was used to synthesize the ZnO nanorods for oxygen detection. The grass-like

nanostructured ZnO sensing layer exhibited a high expose area to the oxygen sample and for UV irradiation. A low-cost UV LED with the wavelength of 370 nm was used to efficiently induced electron carriers in the nanostructured ZnO sensing layer for sensing performance enhancement. The measured resistance of the ZnO sensing layer significantly reduced while UV irradiation, indicating the increase for conductive carriers in the ZnO and the enhanced without using a high working temperature. Results indicated that the developed sensor has a low limit of detection as low as 5 mTorr for detecting oxygen with a short time response of less than 5 min. The calculated variation for three repeating tests for the sensor was around 3.3%, indicating the nice reproducibility for the oxygen sensor. The calculated sensitivities are 0.17(%/mTorr O₂) and 1.83(%/% O₂) for detecting oxygen of different pressures and concentrations, respectively. The developed oxygen sensor has shown its potential to be a high performance oxygen sensor under a low working temperature.

Figure Captions:

Figure 1: Schematic showing the mechanism for enhancing the sensing performance of the nanostructured ZnO oxygen sensor utilizing UV irradiation.

Figure 2: A simplified fabrication process for producing the developed oxygen sensor including the sol-gel and hydrothermal synthesis process.

Figure 3: XRD diffractogram of the synthesized ZnO nanorod after the two-stage sol-gel and hydrothermal processes. Note that the peaks of Au were from the interdigital electrode.

Figure 4: SEM images showing (A) sol-gel grown nanosphere seed-layer, (B) sol-gel grown nanospheres, (C) hydrothermal grown nanorods and (D) the cross-section of the nanorod structure.

Figure 5: The measured sensing responses of ZnO nanorods under various operation temperatures.

Figure 6: The measured sensing responses of various ZnO sensing layers with and without UV irradiation at 50°C.

Figure 7: The measured time response of various ZnO sensing layer with and without UV irradiation at 50°C.

Figure 8: Three repeating tests for detecting 97% of oxygen using the developed oxygen sensor with UV irradiation at 50°C.

Figure 9: (A) The measured step response for detecting oxygen of different pressures. (B) The relationship between the measured responses and the oxygen pressures. (with UV irradiation at 50°C).

Figure 10: (A) The measured step response for detecting oxygen of different concentrations. (B) The relationship between the measured responses and the oxygen concentrations. (with UV irradiation at 50°C)

Reference:

- [1] Q. S. Ding, D. K. Ma, D. L. Li, Y. G. Wei, and N. N. Wen, "A Wireless Control Node for Dissolved Oxygen in Aquaculture," *Sensor Letters*, vol. 11, pp. 1069-1073, Jun-Jul 2013.
- [2] W. C. Maskell, "Inorganic Solid-State Chemically Sensitive Devices - Electrochemical Oxygen Gas Sensors," *Journal of Physics E-Scientific Instruments*, vol. 20, pp. 1156-1168, Oct 1987.
- [3] M. Ryden, E. Cleverstam, A. Lyngfelt, and T. Mattisson, "Waste products from the steel industry with NiO as additive as oxygen carrier for chemical-looping combustion," *International Journal of Greenhouse Gas Control*, vol. 3, pp. 693-703, Dec 2009.
- [4] B. B. Jana and D. Sarkar, "Water quality in aquaculture - Impact and management: A review," *Indian Journal of Animal Sciences*, vol. 75, pp. 1354-1361, Nov 2005.
- [5] H. Minaee, S. H. Mousavi, H. Haratizadeh, and P. W. de Oliveira, "Oxygen sensing properties of zinc oxide nanowires, nanorods, and nanoflowers: The effect of morphology and temperature," *Thin Solid Films*, vol. 545, pp. 8-12, Oct 31 2013.
- [6] G. Korotcenkov, "Metal oxides for solid-state gas sensors: What determines our choice?," *Materials Science and Engineering: B*, vol. 139, pp. 1-23, 2007.
- [7] P. Mitra, A. P. Chatterjee, and H. S. Maiti, "ZnO thin film sensor," *Materials Letters*, vol. 35, pp. 33-38, Apr 1998.
- [8] T. Seiyama, A. Kato, K. Fujiishi, and M. Nagatani, "A New Detector for Gaseous Components Using Semiconductive Thin Films," *Analytical Chemistry*, vol. 34, pp. 1502-1503, 1962.
- [9] O. K. Varghese, D. Gong, M. Paulose, K. G. Ong, and C. A. Grimes, "Hydrogen sensing using titania nanotubes," *Sensors and Actuators B: Chemical*, vol. 93, pp. 338-344, 2003.
- [10] P. Hu, G. Du, W. Zhou, J. Cui, J. Lin, H. Liu, *et al.*, "Enhancement of ethanol vapor sensing of TiO₂ nanobelts by surface engineering," *Acs Applied Materials & Interfaces*, vol. 2, pp. 3263-3269, 2010.
- [11] L. FRANCIOSO, A. TAURINO, A. FORLEO, and P. SICILIANO, "TiO₂ nanowires array fabrication and gas sensing properties," *Sensors and actuators. B, Chemical*, vol. 130, pp. 70-76, 2008.
- [12] D. WANG, X. CHU, and M. GONG, "Gas-sensing properties of sensors based on single-crystalline SnO₂ nanorods prepared by a simple molten-salt method," *Sensors and actuators. B, Chemical*, vol. 117, pp. 183-187, 2006.
- [13] J.-K. Choi, I.-S. Hwang, S.-J. Kim, J.-S. Park, S.-S. Park, U. Jeong, *et al.*, "Design of selective gas sensors using electrospun Pd-doped SnO₂ hollow nanofibers," *Sensors and Actuators B: Chemical*, vol. 150, pp. 191-199, 2010.
- [14] T. LE VIET, N. D. HOA, D. T. T. LE, V. DO THANH, P. D. TAM, A.-T. LE, *et al.*, "On-chip fabrication of SnO₂-nanowire gas sensor: The effect of growth time on sensor performance," *Sensors and actuators. B, Chemical*, vol. 146, pp. 361-367, 2010.
- [15] X. Lu and L. Yin, "Porous Indium oxide nanorods: Synthesis, characterization and gas sensing properties," *Journal of Materials Science & Technology*, vol. 27, pp. 680-684, 2011.
- [16] W. Zheng, X. Lu, W. Wang, Z. Li, H. Zhang, Z. Wang, *et al.*, "Assembly of Pt

- nanoparticles on electrospun In₂O₃ nanofibers for H₂S detection," *Journal of colloid and interface science*, vol. 338, p. 366, 2009.
- [17] R. Sharma, M. Bhatnagar, and G. Sharma, "Mechanism of highly sensitive and fast response Cr doped TiO₂ oxygen gas sensor," *Sensors and Actuators B: Chemical*, vol. 45, pp. 209-215, 1997.
- [18] A. Kolmakov, D. Klenov, Y. Lilach, S. Stemmer, and M. Moskovits, "Enhanced gas sensing by individual SnO₂ nanowires and nanobelts functionalized with Pd catalyst particles," *Nano Letters*, vol. 5, pp. 667-673, 2005.
- [19] H.-T. Wang, B. Kang, F. Ren, L. Tien, P. Sadik, D. Norton, *et al.*, "Hydrogen-selective sensing at room temperature with ZnO nanorods," *Applied Physics Letters*, vol. 86, pp. 243503-243503-3, 2005.
- [20] X. Xue, L. Xing, Y. Chen, S. Shi, Y. Wang, and T. Wang, "Synthesis and H₂S Sensing Properties of CuO– SnO₂ Core/Shell PN-Junction Nanorods," *The Journal of Physical Chemistry C*, vol. 112, pp. 12157-12160, 2008.
- [21] S. SI, C. LI, X. WANG, Q. PENG, and Y. LI, "Fe₂O₃/ZnO core-shell nanorods for gas sensors," *Sensors and actuators. B, Chemical*, vol. 119, pp. 52-56, 2006.
- [22] N. VAN HIEU, H.-R. KIM, B.-K. JU, and J.-H. LEE, "Enhanced performance of SnO₂ nanowires ethanol sensor by functionalizing with La₂O₃," *Sensors and actuators. B, Chemical*, vol. 133, pp. 228-234, 2008.
- [23] Z. Guo, M. Li, and J. Liu, "Highly porous CdO nanowires: preparation based on hydroxy-and carbonate-containing cadmium compound precursor nanowires, gas sensing and optical properties," *Nanotechnology*, vol. 19, p. 245611, 2008.
- [24] G. Wang, J. Park, M. Park, and X. L. Gou, "Synthesis and high gas sensitivity of tin oxide nanotubes," *Sensors and Actuators B: Chemical*, vol. 131, pp. 313-317, 2008.
- [25] H. Yu and M. Choi, "Electrical and CO gas sensing properties of ZnO-SnO₂ composites," *Sensors and Actuators B: Chemical*, vol. 52, pp. 251-256, 1998.
- [26] Y.-J. Chen, C.-L. Zhu, L.-J. Wang, P. Gao, M.-S. Cao, and X.-L. Shi, "Synthesis and enhanced ethanol sensing characteristics of α -Fe₂O₃/SnO₂ core-shell nanorods," *Nanotechnology*, vol. 20, p. 045502, 2009.
- [27] S. Q. Tian, X. H. Ding, D. W. Zeng, J. J. Wu, S. P. Zhang, and C. S. Xie, "A low temperature gas sensor based on Pd-functionalized mesoporous SnO₂ fibers for detecting trace formaldehyde," *Rsc Advances*, vol. 3, pp. 11823-11831, 2013.
- [28] A. Janotti and C. G. Van de Walle, "Fundamentals of zinc oxide as a semiconductor," *Reports on Progress in Physics*, vol. 72, Dec 2009.
- [29] D. Gedamu, I. Paulowicz, S. Kaps, O. Lupan, S. Wille, G. Haidarschin, *et al.*, "Rapid Fabrication Technique for Interpenetrated ZnO Nanotetrapod Networks for Fast UV Sensors," *Advanced Materials*, vol. 26, pp. 1541-1550, Mar 2014.
- [30] R. Gurwitz, R. Cohen, and I. Shalish, "Interaction of light with the ZnO surface: Photon induced oxygen "breathing," oxygen vacancies, persistent photoconductivity, and persistent photovoltage," *Journal of Applied Physics*, vol. 115, Jan 21 2014.
- [31] N. Sakai, Y. Ebina, K. Takada, and T. Sasaki, "Photocurrent generation from semiconducting manganese oxide nanosheets in response to visible light," *J Phys Chem B*, vol. 109, pp. 9651-5, May 19 2005.
- [32] L. Peng, Q. Zhao, D. Wang, J. Zhai, P. Wang, S. Pang, *et al.*, "Ultraviolet-assisted gas sensing: a potential formaldehyde detection approach at room temperature based on zinc oxide nanorods," *Sensors and Actuators B: Chemical*, vol. 136, pp. 80-85, 2009.
- [33] S.-W. Fan, A. K. Srivastava, and V. P. Dravid, "Nanopatterned polycrystalline ZnO for room temperature gas sensing," *Sensors and Actuators B: Chemical*, vol. 144, pp.

- 159-163, 2010.
- [34] L. Ji, S. Peng, Y.-K. Su, S.-J. Young, C. Wu, and W. Cheng, "Ultraviolet photodetectors based on selectively grown ZnO nanorod arrays," *Applied Physics Letters*, vol. 94, pp. 203106-203106-3, 2009.
- [35] O. Lupan, L. Chow, and G. Y. Chai, "A single ZnO tetrapod-based sensor," *Sensors and Actuators B-Chemical*, vol. 141, pp. 511-517, Sep 7 2009.
- [36] B. M. Rajbongshi and S. K. Samdarshi, "ZnO and Co-ZnO nanorods-Complementary role of oxygen vacancy in photocatalytic activity of under UV and visible radiation flux," *Materials Science and Engineering B-Advanced Functional Solid-State Materials*, vol. 182, pp. 21-28, Mar 2014.
- [37] O. Lupan, T. Pauporte, L. Chow, B. Viana, F. Pelle, L. K. Ono, *et al.*, "Effects of annealing on properties of ZnO thin films prepared by electrochemical deposition in chloride medium," *Applied Surface Science*, vol. 256, pp. 1895-1907, Jan 1 2010.
- [38] H.-U. Lee, K. Ahn, S.-J. Lee, J.-P. Kim, H.-G. Kim, S.-Y. Jeong, *et al.*, "ZnO nanobarbed fibers: Fabrication, sensing NO₂ gas, and their sensing mechanism," *Applied Physics Letters*, vol. 98, p. 193114, 2011.
- [39] M. Yang, T. Xie, L. Peng, Y. Zhao, and D. Wang, "Fabrication and photoelectric oxygen sensing characteristics of electrospun Co doped ZnO nanofibres," *Applied Physics A*, vol. 89, pp. 427-430, 2007.
- [40] S. Hung, C.-J. Chung, C. C. Chen, C. Lo, F. Ren, S. Pearton, *et al.*, "SnO₂-gated AlGa_N/Ga_N high electron mobility transistors based oxygen sensors," *Journal of Vacuum Science & Technology B*, vol. 30, 2012.
- [41] C. Cava, R. Salvatierra, D. Alves, A. Ferlauto, A. Zarbin, and L. Roman, "Self-assembled films of multi-wall carbon nanotubes used in gas sensors to increase the sensitivity limit for oxygen detection," *Carbon*, vol. 50, pp. 1953-1958, 2012.

Figure 1

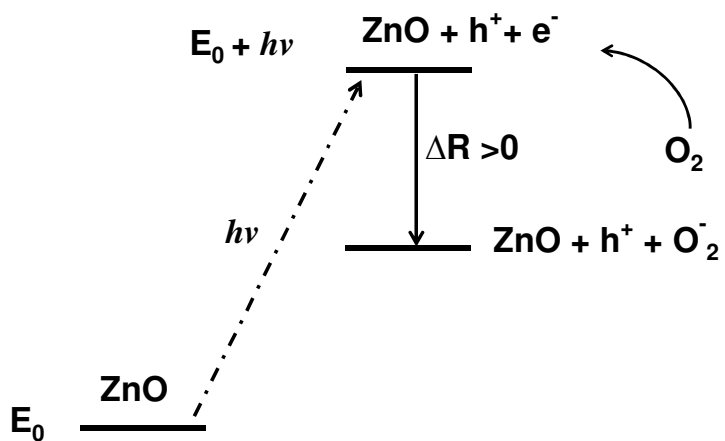


Figure 1: Schematic showing the mechanism for enhancing the sensing performance of the nanostructured ZnO oxygen sensor utilizing UV irradiation.

Figure 2

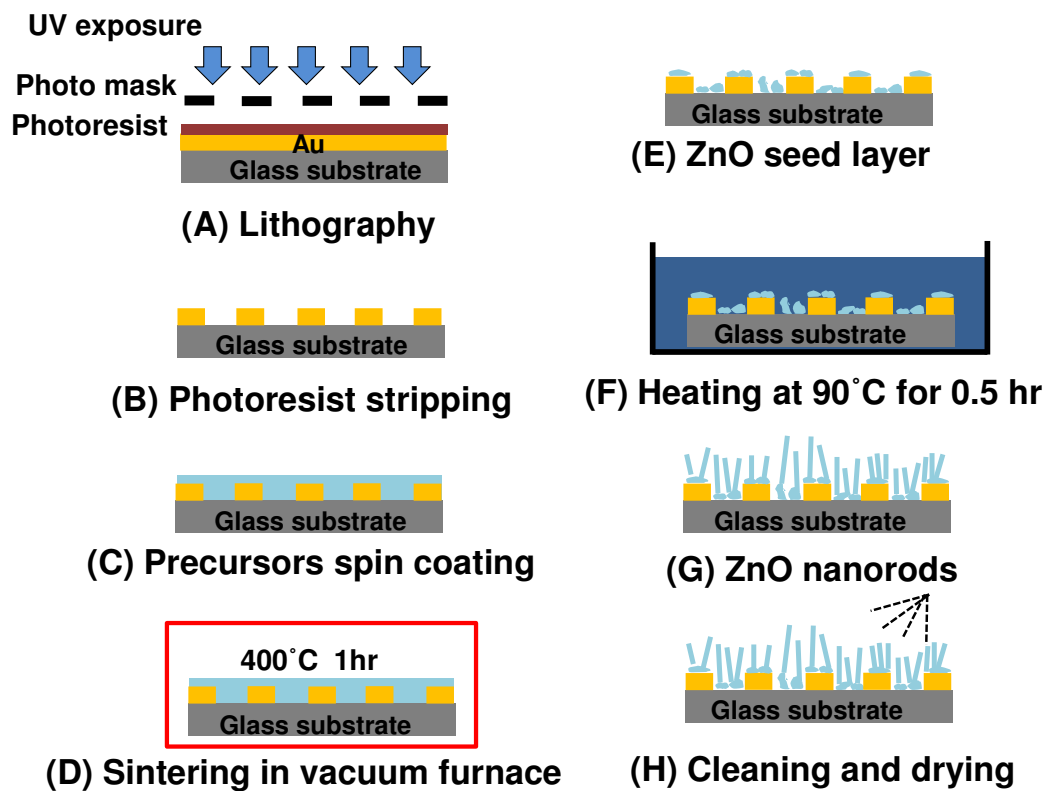


Figure 2: A simplified fabrication process for producing the developed oxygen sensor including the sol-gel and hydrothermal synthesis process.

Figure 3

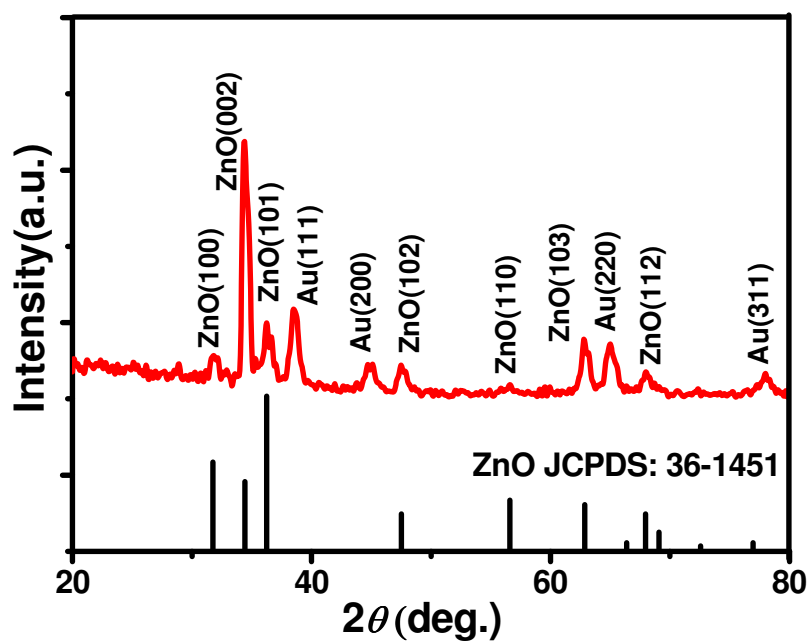


Figure 3: XRD diffractogram of the synthesized ZnO nanorod after the two-stage sol-gel and hydrothermal processes. Note that the peaks of Au were from the interdigital electrode.

Figure 4

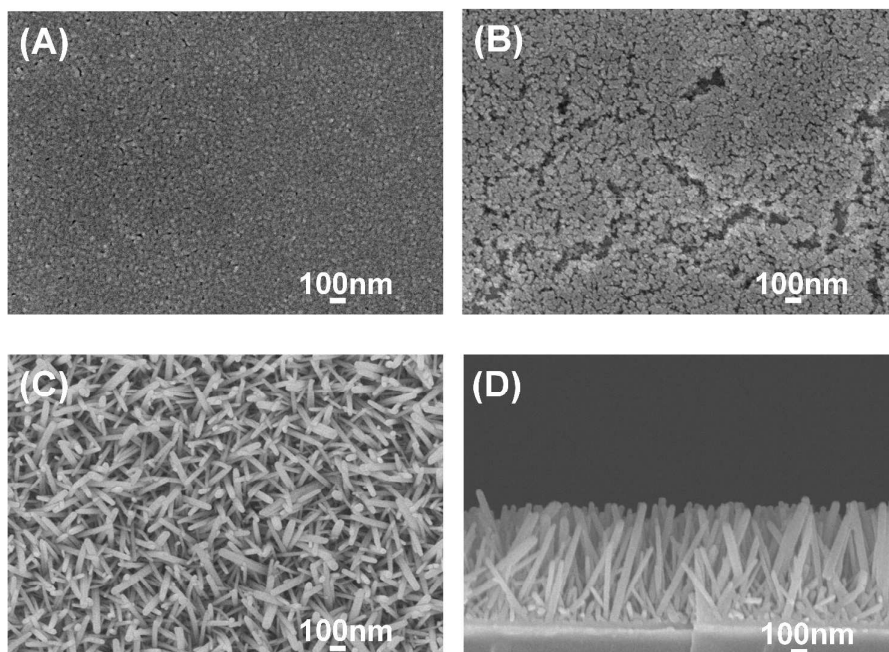


Figure 4: SEM images showing (A) sol-gel grown nanospheres seed-layer, (B) sol-gel grown nanospheres, (C) hydrothermal grown nanorods and (D) the cross-section of the nanorod structure.

Figure 5

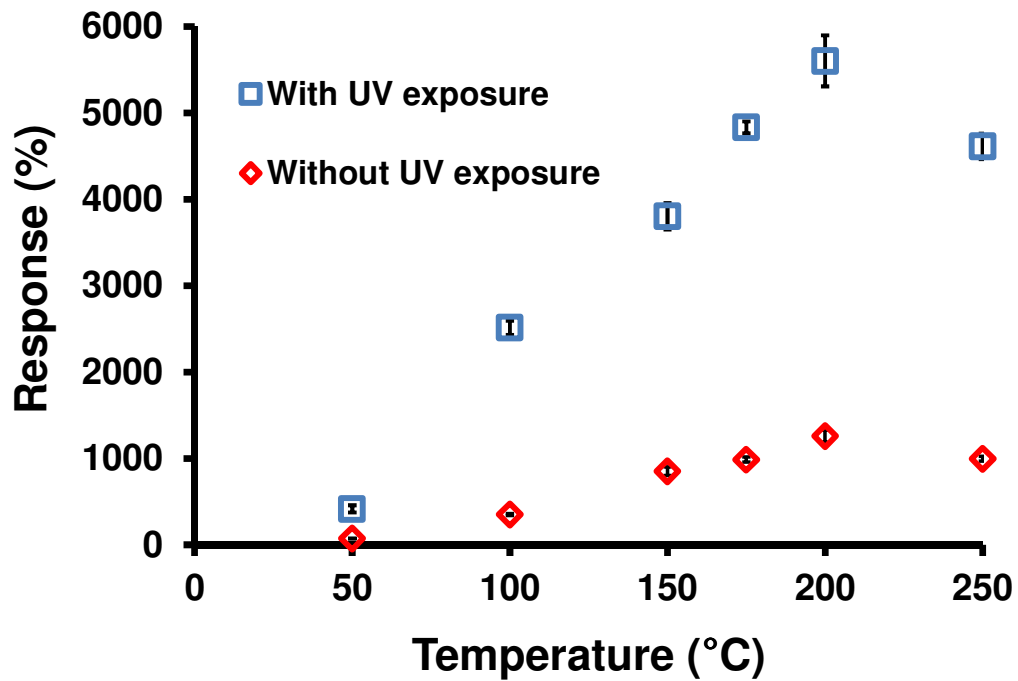


Figure 5: The measured sensing responses of ZnO nanorods under various operation temperatures.

Figure 6

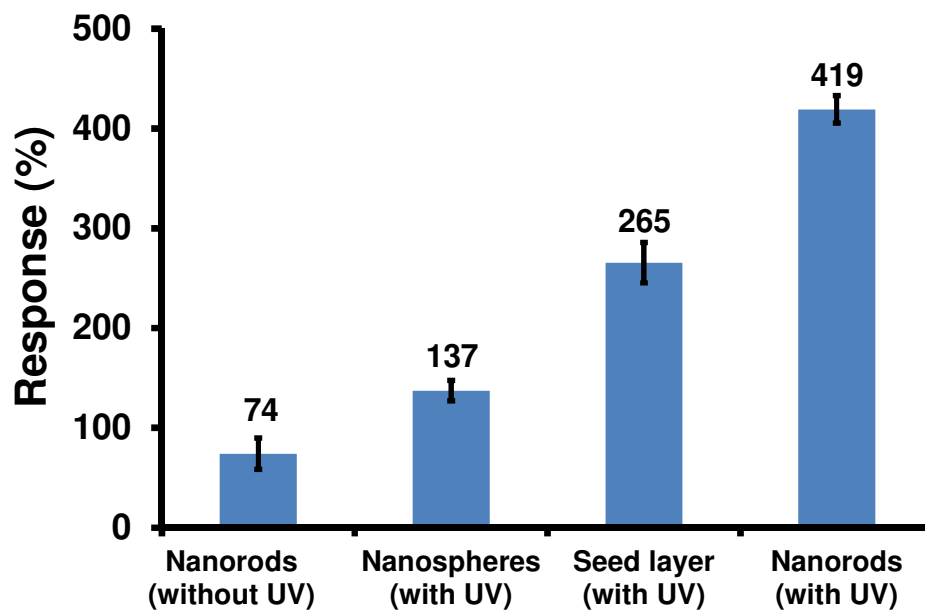


Figure 6: The measured sensing responses of various ZnO sensing layers with and without UV irradiation at 50°C.

Figure 7

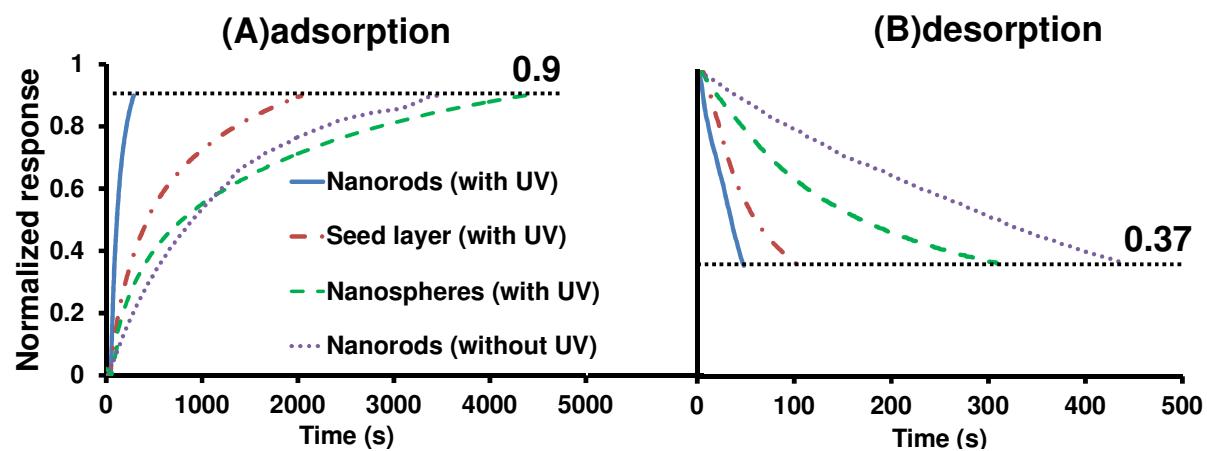


Figure 7: The measured time response of various ZnO sensing layer with and without UV irradiation at 50°C.

Figure 8

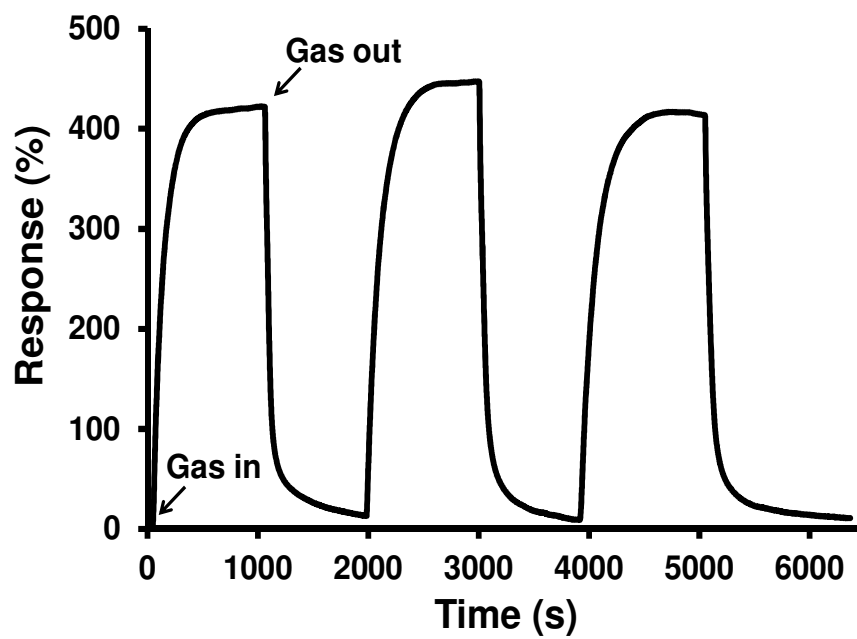


Figure 8: Three repeating tests for detecting 97% of oxygen using the developed oxygen sensor with UV irradiation at 50°C.

Figure 9

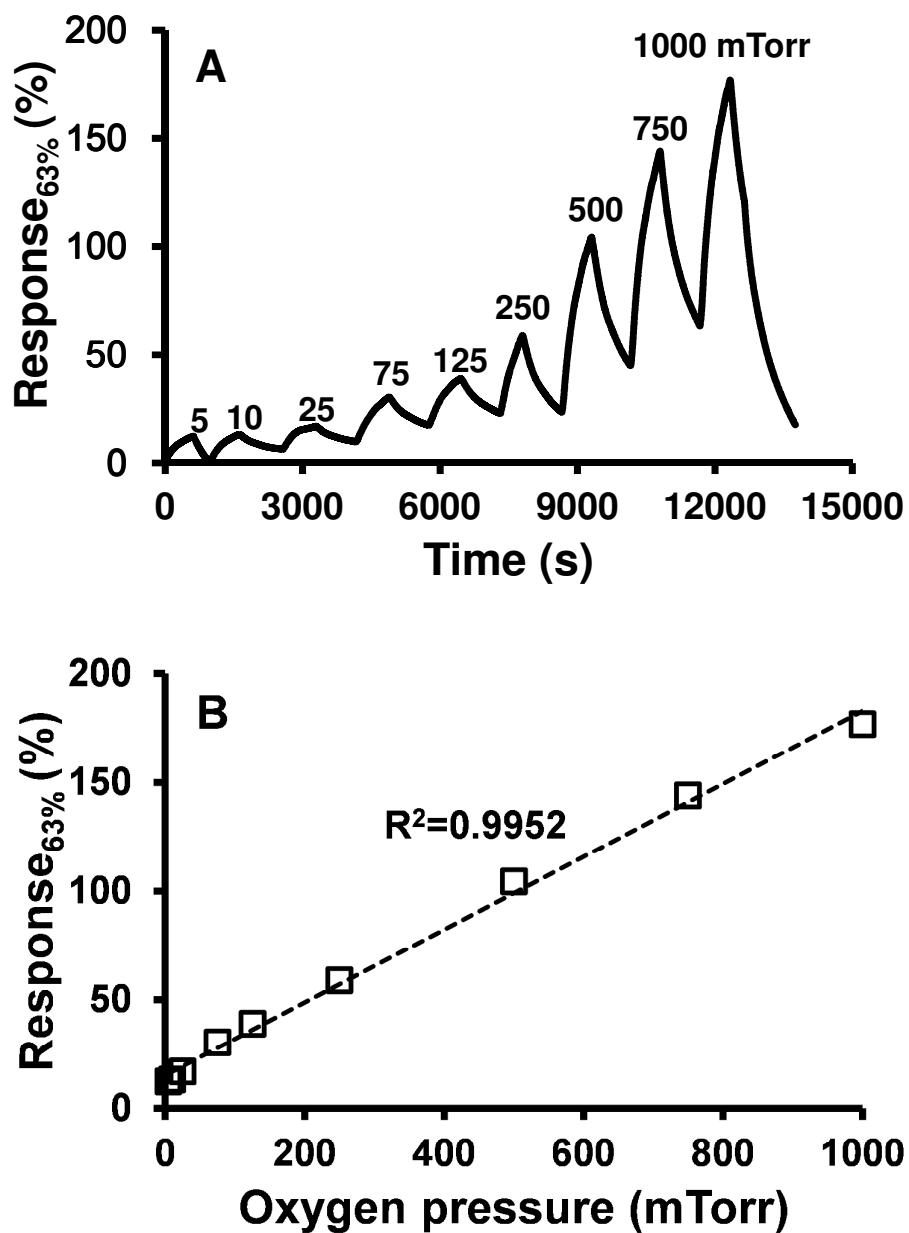


Figure 9: (A) The measured step response for detecting oxygen of different pressures. (B) The relationship between the measured responses and the oxygen pressures. (with UV irradiation at 50°C).

Figure 10

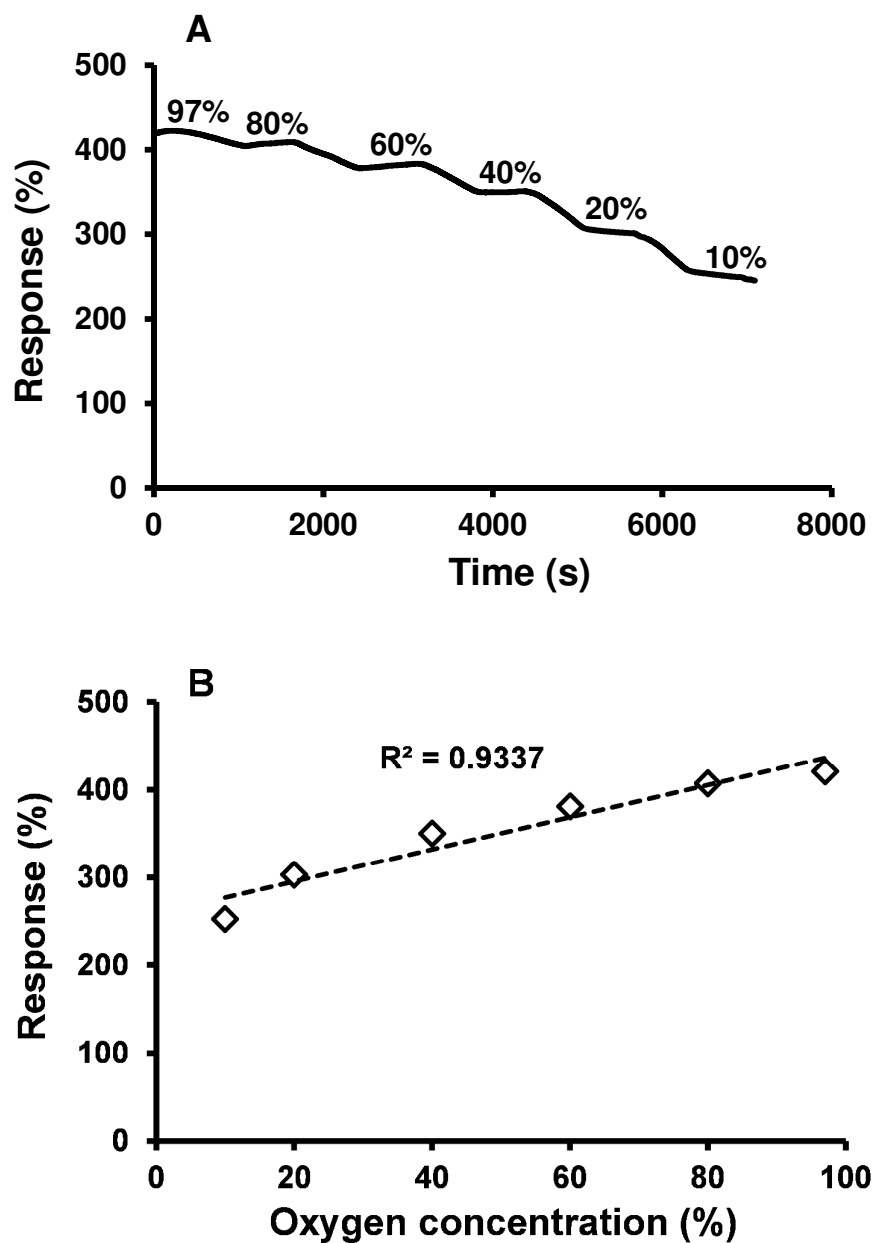


Figure 10: (A) The measured step response for detecting oxygen of different concentrations. (B) The relationship between the measured responses and the oxygen concentrations. (with UV irradiation at 50°C)